crystals

MDPI

*Review*

# Review of the Strengthening Methods and Mechanical Properties of Recycled Aggregate Concrete (RAC)

**Chuanqi Liu [1,2], Yanjun Wang [3], Xuyang Gao [2], Guanglong Zhang [4], Heng Liu [5], Chong Ma [2], Jilin Sun [2] and Jinxing Lai [1,*]**

1 School of Highway, Chang'an University, Xi'an 710064, China
2 Department of Civil Engineering, Qingdao University of Technology, Qingdao 266000, China
3 Linyi Municipal Engineering Construction Management Service Center, Linyi 276000, China
4 Shandong High Speed Engineering Testing Co., Ltd., Jinan 250000, China
5 Shandong Construction Engineering Quality Inspection and Testing Center Co., Ltd., Jinan 250000, China
* Correspondence: laijinxing@chd.edu.cn

**Abstract:** Replacing natural aggregate (NA) with recycled aggregate (RA) has contributed to the trend of sustainable development in civil construction. With this background, improvements in the mechanical properties of recycled aggregate concrete (RAC) and the scientific design of the mixture ratio are attracting more concern in recent years. This paper is a review of the recent research, including the following aspects: the mixture design of RAC; the improved mechanical properties of recycled concrete with steel fibers; and the performance of the main components. In addition, the primary composition materials, properties, and calculation methods of the mixture ratio of RAC are summarized. The mechanical properties, durability and microscopic analysis of RAC are also discussed. The accurate calculation of mixture proportion can significantly facilitate the work of preparing a test mix of RAC. Through the mixture-ratio optimization and physical and chemical strengthening of RA, the mechanical properties of RAC can be improved to promote the wider application of this eco-friendly material.

**Keywords:** recycled aggregate concrete; mixture proportion design; steel fibers; mechanical properties; eco-friendly material



**Citation:** Liu, C.; Wang, Y.; Gao, X.; Zhang, G.; Liu, H.; Ma, C.; Sun, J.; Lai, J. Review of the Strengthening Methods and Mechanical Properties of Recycled Aggregate Concrete (RAC). *Crystals* **2022**, *12*, 1321. https://doi.org/10.3390/cryst12091321

Academic Editors: Amjad Albayati and Zongyou Yin

Received: 6 July 2022
Accepted: 23 August 2022
Published: 19 September 2022



## 1. Introduction

Fast urbanization has brought huge amounts of material costs as well as waste building materials (mainly concrete). Waste concrete blocks are crushed to replace natural aggregates (NAs) and are mixed with concrete materials to realize sustainable uses of building materials, saving energy and reducing carbon emissions [1–4]. Different from NA, the outer layer of the RAC is covered by cement mortar [5,6], which has some unique disadvantages, such as a high water-absorption rate, low density, low-strength, and poor bond strength with cementing materials [7,8]. Recycled aggregate (RA) consists of crushed solid waste from buildings. RA has many edges and corners and a large proportion of flaky material.

There are many shortcomings of RA, therefore improving the mechanical properties of RAC has become an interesting topic. To address this problem, physical and chemical strengthening of the RA is commonly performed [9–11]. Physical strengthening refers to the removal of the cement mortar and the edges and corners on the surface of the RA through impact and friction using mechanical means [12,13].Chemical strengthening refers to the use of certain active grouts or chemical agents to fill pores and cracks in the RA [14–16]. Besides, steel fibers (SFs) can be added to improve the mechanical properties of RAC [17–22], such as tensile, crack-resistance, and bending properties.

In addition to the above strengthening methods, an appropriate and accurate mixed-ratio design is also important to ensure the good mechanical performance of RAC. The compressive strength of concrete in RAC is 20–25% lower than that of natural aggregate concrete (NAC) with the same mixing ratio [23–25]. The properties and substitution rate of the recycled aggregate (RA) determine the compressive strength of the RAC [26,27]. The requirement of low-strength concrete (20 MPa) can be met by RA, but for RAC to be widely used, it must meet the requirements of medium-strength concrete (40 MPa) and high-strength concrete (60 MPa).

In this paper, the mixture proportion design methods of RAC are reviewed. The technical route of the mixture proportion design and the use of orthogonal experimental methods are introduced. In addition, the function and composition of various materials of RAC, the material content in the test, and the calculation methods are reviewed. The purpose of this review is to improve the accuracy and universal application of the RAC mixture-ratio design.

## 2. Technical Route of RAC Mix Design

The mixed-proportion design of concrete is the basis of research on RAC, which determines the compressive strength, flexural performance, and durability of RAC, and directly affects the application and promotion of RAC. In the weight-replacement method, RAC is prepared by the mixed-proportion design method of NAC, then the NA is replaced by some RA or all RA. The results showed that the performance of RAC prepared by the weight-replacement method was worse than that of NAC, with the same mix proportion. RA was used as a coarse aggregate, and the compressive strength of RAC was 5–24% lower than that of NAC [28]. When RA was used in both coarse and fine aggregates, the compressive strength of RAC was 15–40% lower than that of NAC [29]. This is because the water absorption of RCA is greater than that of NA, and the crushing index is greater than that of NA. According to the characteristics of the high water absorption of RCA, the influence of high water absorption of RA on the working performance of RAC was reduced by pre-wetting water and increasing compensation water [28,29], and the strength of RAC then increased by about 20% [30,31]. With regard to the equivalent cement volume method, Koenders, E.A.B et al. [32] proposed the mixed-design method of RAC with an equivalent cement volume. ///RA is a composite material composed of NA and cement mortar. When designing the mix proportion of RAC, the amount of NA and cement mortar in RAC should be the same as that in NAC. This could ensure that the mechanical properties of the RAC were the same as those of the NAC under the same mix proportion, but the equivalent cement volume method in this situation does not take into account that the small-size RA was only composed of mortar and cement, and the compressive strength of the RAC prepared in this case was low. Pepe M. et al. [33] put forward the mixed-design method with the water absorption of RA as the main parameter. By studying the parameters, the effective water-binder ratio of RAC was calculated, and the compressive strength, flexural performance, and durability of RAC were predicted. Lijuan Zhang et al. [34] used the orthogonal test method to analyze the significance of steel fiber RAC, and discovered that the volume ratio of steel fiber and the replacement rate of RA had a significant impact on the slump and the water-cement ratio; additionally, the replacement rate of RA had a significant impact on the compressive strength and the water-cement ratio and the volume ratio of steel fiber had a significant impact on the splitting tensile strength. On the basis of orthogonal tests, through a large number of mixed-proportion tests and theoretical analysis and fitting the experimental data, the mixed-proportion design method suitable for steel fiber RAC was established. An orthogonal experimental design is a multi-factor and multi-level design method [32,33]. According to the orthogonality, representative points are selected from a comprehensive test. The representative points have the characteristics of uniform dispersion, uniformity, and comparability. The orthogonal experimental design is a fractional factor design method and is efficient, rapid, and economical. Takeuchi, a famous Japanese statistician, listed the horizontal combinations obtained in orthogonal experiments in an orthogonal table.

## 3. Method to Improve Performance of RAC and Determine the Dosage of Composition Material

RAC mainly consists of cement, sand, NA, RA, water, and superplasticizer. As for SF recycled concrete, the amount of SF depends on the amount of recycled concrete material. The amounts and accelerating agent (AG) depend on the amount of SF. Self-compacting recycled concrete, fly ash, and silicon powder (SP) are added on the basis of recycled concrete materials. The material composition is shown in Figure 1, and the chemical composition of the main materials is shown in Table 1.

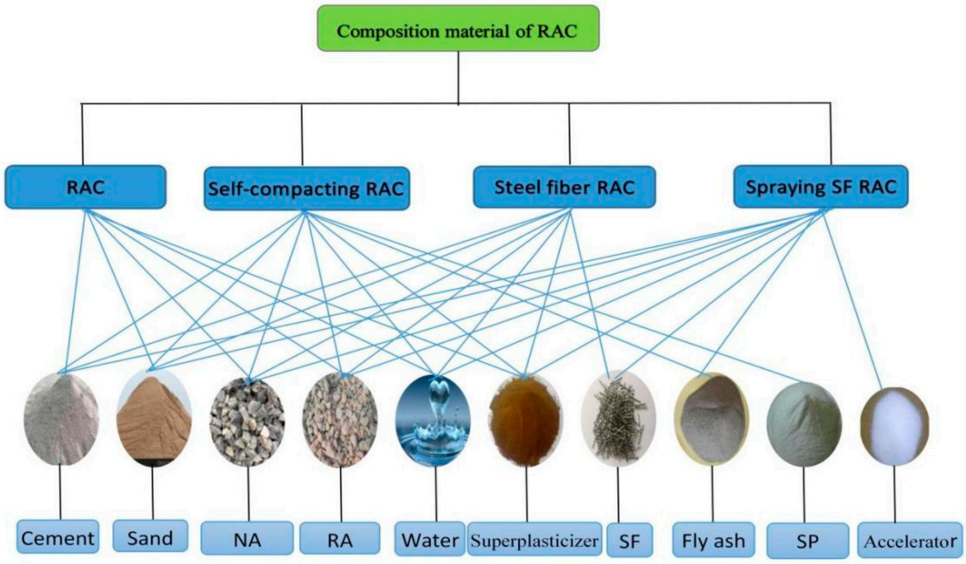


**Figure 1.** Composition materials of RAC.

**Table 1.** Composition of the basic constituent materials, such as cement, and industrial residue.

| Classification | Type | Composition | Ref. |
|---|---|---|---|
| Cement | Portland cement | Major ($C_3S$, $C_2S$, $C_3A$, $C_4AF$); minor ($CaSO_4$) | [35] |
| | Sulphoaluminate cement | Major ($C_4A_3$, $Al_2O_3$, CaO, $SiO_2$, $C_2S$, $SO_3$); minor ($C_4AF$, $Fe_2O_3$) | [36] |
| Industrial residue | Fly ash | Major ($SiO_2$, $Al_2O_3$, CaO, $Fe_2O_3$, MgO, $SO_3$); minor ($Na_2O$, $K_2O$) | [37] |
| | Silica fume | Major ($SiO_2$, $Al_2O_3$, $Fe_2O_3$); minor (MgO, CaO, $Na_2O$) | [37] |

### *3.1. Recycled Aggregate (RA)*

The use of crushed building concrete waste to replace the NA in concrete partially or entirely and the pouring of concrete in construction are conducive to the green and sustainable development of the civil engineering field; there exists significant market demand and considerable prospects for this product [38–47]. Japan, the United States, Germany, and other countries began early development of RAC utilization, and developed relevant technical standards and specifications for RAC, as summarized in Table 2.

**Table 2.** Summary of standards and specifications for recycled concrete in various countries.

| Countries | Year | Technical Standards | Note |
|---|---|---|---|
| Japan | 1977 | Technical standard for recycled concrete | First put forward |
| United States | 1982 | ASTMC-33-82 | Removal of restrictions on the application of recycled aggregate in construction projects |
| Germany | 1988 | Guidelines for the application of reclaimed aggregate in concrete | The recycled aggregate is divided into 4 grades |

**Table 2.** *Cont.*

| Countries | Year | Technical Standards | Note |
|---|---|---|---|
| South Korea | 2003 | Construction waste regeneration promotion method | The use and obligations of the relevant producers for recycled aggregate are clarified |
| Japan | 2005–2007 | JISA5021, JISA5022, JISA5023 | The country's construction sector is highly leveraged |
| China | 2012 | Suggestions on the transportation management of earthwork sand and gravel for construction garbage | Detailed rules have been drawn up for the management of construction waste in China |

3.1.1. Treatment of RA

Since the surface of RA is covered with cement mortar, compared with NA it has large surface pores and a high water-absorption capacity. The compressive strength of concrete in RA is 20–25% lower than that of NAC with the same mix ratio [22,47–50]. The quality of RA and its replacement rate directly affect the compressive strength of concrete [51,52]. Chemical and physical treatments were conducted to reduce the porosity and water-absorption capacity of RAC. Bui et al. [53] used a sodium silicate solution to treat RA and added SP to improve its performance, and It was found that this could increase the compressive strength by 33 – 50%. Wang et al. [54] immersed RA in an acetic acid solution and observed the reaction of the cement compound bonded to the RA: the treated cement mortar covered by the treated aggregate was easily removed by mechanical friction, improving compressive strength by up to 25%. Saravanakumar et al. [49] soaked RA with HCL, $H_2SO_4$, $HNO_3$, and a mixed solution of hydrochloric acid and SP. It was found that this treatment improved the physical and mechanical properties of RAC significantly and could improve compressive strength by 8–18% at the age of 28 days, compared with untreated RAC. Zhan et al. [50] used a carbonation process to reduce the water-absorption rate and improve the density of RA. Ismail et al. [16] treated RA with a low-concentration acid solution and found that it significantly improved the physical and mechanical properties of RA, which could achieve a compressive strength of up to or above 50 Mpa at 28 days. Gupta et al. [51] used a freeze-thaw cycle to treat RA, which stripped the cement mortar from the RA to improve its performance, as shown in Figure 2.

(**a**) (**b**) (**c**)

**Figure 2.** Recycled aggregate is treated using freezing-thawing cycles. (**a**) The sample of frozen RA; (**b**) Remove aggregate mortar; (**c**) Treated recycled aggregate.

3.1.2. Amount of RA

The calculation of the amount of RA is based on the amount of NA to determine the replacement rate of RA ($r_g$). There is no clear industry standard for the replacement rate of RA. The volume formula is used to calculate the amount of the aggregate: $m_g$, $m_{ra} = r_g * m_g$. Equation (1) is used in the standard JGJ52-2006 [52], Volume formula: the sum of the volumes of the concrete constituent materials is 1.

### 3.2. Steel Fiber

The tensile, splitting, and deformation resistance of concrete can be significantly improved by adding SF to the concrete. The addition of SF to concrete changes the stress concentration point of the microcracks and inhibits the development and propagation of delayed microcracks. Concrete is a brittle material, and SF evenly dispersed into concrete has a reinforcing and softening effect, and improves the performance of concrete. Many scholars have used the addition of SF to improve the mechanical properties of RAC.

#### 3.2.1. Crack Resistance Theory of Steel Fiber

When concrete shrinks, external constraints prevent the shrinkage and deformation of the concrete, and tensile stress occurs inside the concrete, as shown in Figure 3. When the tensile stress reaches the tensile stress limit of the concrete, the micro-cracks inside the concrete expand and form large cracks. When SF is mixed with the concrete, the soil around the original microfracture and the SF and concrete interface bond change the stress concentration point of the microfracture. As for the tensile stress, a stress field occurs inside the concrete, causing cracks to appear. When the tensile strength of the concrete reaches the limit, the tensile stress in the SF is transmitted to the uncracked portion. A new crack appears, but the fiber concrete does not break [53–55], as shown in Figure 3a.

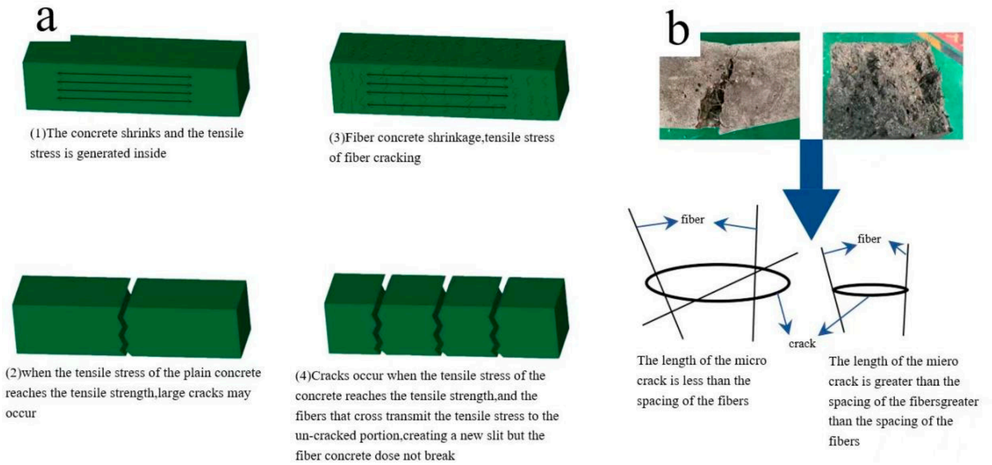


**Figure 3.** Crack resistance mechanism of steel fiber. (**a**) Crack resistance mechanism of steel fiber when concrete is under tension. (**b**) Crack resistance mechanism of steel fiber with different lengths of micro-cracks).

The SF exists in the form of a linear aggregate in the concrete and prevents the formation of internal micro-cracks as the concrete shrinks and deforms. When the length of the micro-crack is larger than the distance between the SFs, the SFs transfer the load of the micro-crack load and distribute the stress load evenly. Thus, the stress of the micro-crack is concentrated on the tip and is passivated, limiting further expansion of the micro-crack. When the length of the micro-crack is less than the distance between the SFs, the SFs prevent the expansion of micro-cracks and force the micro-cracks to change their path. Thus, the internal energy of the micro-crack is dispersed and the development of micro-cracks is prevented [55], as shown in Figure 3b.

#### 3.2.2. Composite Mechanical Reinforcement Theory of Steel Fiber

The British researchers Samy et al. and the American researcher Naaman first used the theory of composite mechanics to investigate SF reinforced concrete. In SF reinforced concrete or SF recycled concrete, the SF is regarded as one phase of the fiber reinforcement system, and the concrete or recycled concrete is the other phase in the theory of composite mechanics. The combination of the materials results in composite materials. The overall mechanical properties of the composite material are the sum of the mechanical properties of the two materials [55].

The basic assumptions of composite mechanics are shown in Figure 4: (1) The SFs are arranged in parallel and uniformly in the concrete, and are in the same direction as the concrete stress. (2) The SFs and concrete have no relative slip, and the strain is equal $\varepsilon_c = \varepsilon_m = \varepsilon_f$. (3) Both the SFs and the concrete are in elastic deformation, and the deformation is consistent: $f_c = \sigma_c * A_c$, $f_m = \sigma_m * A_m$, $f_f = \sigma_f * A_f$ $f_c$, $f_m$, $f_f$ representing the total load of the composite matrix, the concrete, and the SF, respectively. $\sigma_c$, $\sigma_m$, $\sigma_f$ represent the stress of the composite matrix, the concrete, and the SF, respectively. $A_c$, $A_m$, $A_f$ represent the cross-sectional area of the composite matrix, the concrete, and the SF, respectively. Since the elastic modulus of the SF is far greater than that of the concrete, when the composite matrix is subjected to stress and deformation the SF improves the mechanical properties of the concrete or RAC [55].

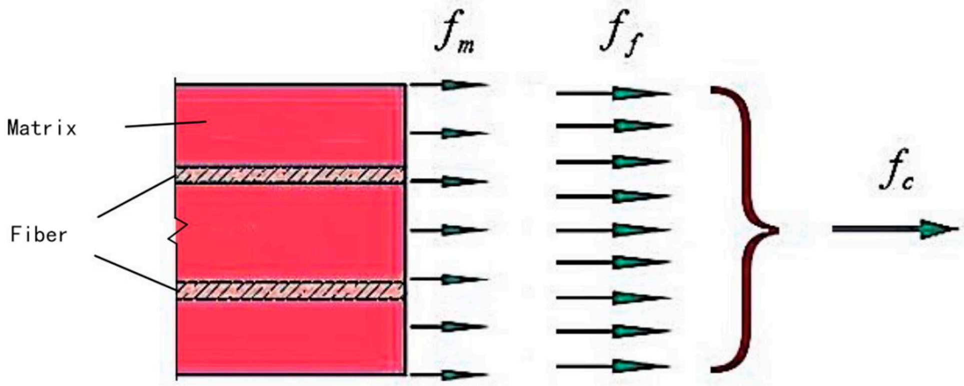


**Figure 4.** Mechanical reinforcement mechanism of steel fiber composite material.

### 3.2.3. Theoretical Mechanical Reinforcement of Steel Fiber Spacing

Romualdi et al. put forward the SF spacing theory in 1963, and used the theory of fracture mechanics in the analysis of SF reinforced concrete. Concrete is a brittle material, with internal micro-cracks, and the adding of SF significantly reduces the number of micro-cracks and disperses their stress concentration. Romualdi used the theory of forward continuous SF concrete and assumed that the SFs were evenly distributed in the concrete in the form of a chessboard, and were oriented in the direction of the pull. Cracks occurred in the center of the area surrounded by the SFs under the action of tensile stress. Bond stress occurred around the fiber, and opposite stress was produced at the tip of the cracks; the SFs prevented the generation of cracks and improved the mechanical properties of the concrete or recycled concrete [55–60].

### 3.2.4. Steel Fiber Content

The SF reinforcement theory summarized in the above Sections 3.2.1–3.2.3 indicates the feasibility of adding SF to RAC to improve the performance of recycled concrete. The properties of the concrete matrix are generally improved with an increase in the SF volume ratio, but it is necessary to consider whether the SFs are uniformly dispersed in the concrete, and the volume ratio of the SFs should not exceed 2% [61]. The significance analysis of RAC in the orthogonal experiment indicates that the SF content has a significant influence on the crack resistance and flexural strength of RAC. Gao [62] fitted the formula of the relationship between the flexural strength of RAC and the SF content, as shown in Figure 5 and Equations (2) and (3). The volume ratio of SFs can be calculated based on the length and diameter of the SF. However, the tensile strength of the SF is not considered in this formula. During a splitting test of SF-RA, some SFs were pulled apart. Ma [63] fitted the relationship between the splitting strength of sprayed SF concrete and the volume ratio of the SF while considering the tensile strength of the SF, as shown in Equation (4). This equation is an important reference for the calculation of the volume ratio of SFs in RAC. In this manner, the volume of the SF can be calculated according to the design value of the splitting strength of SF shotcrete and the design value of different tensile strengths of the SF.

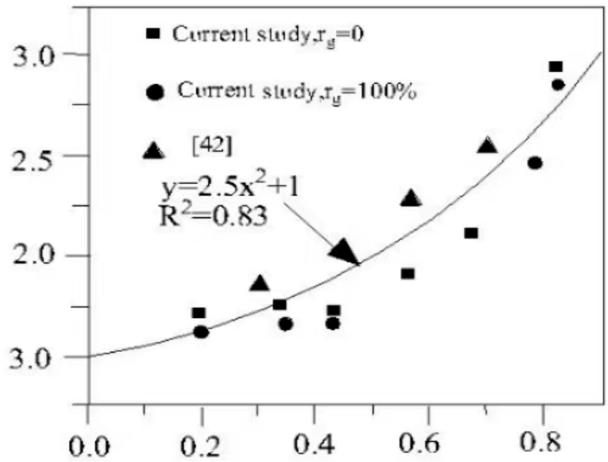


**Figure 5.** Relationship between the steel fiber content in steel fiber recycled concrete and the flexural strength [61].

*3.3. Water/Cement Ratio*

At the same replacement rate of RA ($r_g$), the compressive strength of RAC decreases with an increase in the water/cement ratio. A decrease of water-cement ratio increases the compressive strength of RAC. However, a simple reduction of the water-cement ratio will lead to poor workability of the RAC. In engineering applications, a water-reducing agent is generally added to reduce the water-binder ratio and improve the compressive strength of the concrete without affecting its workability. The water-cement ratio has a constant linear relationship with the compressive strength and the cement strength of the concrete. The relationship is generally fitted by the empirical Equation (5). This is associated with factors such as the type of cement and aggregate, and can be determined by fitting the experimental data. Li et al. [64] developed the concept of the absolute hydrogel mass ratio, as introduced in Equation (6). Gao et al. [62] fitted Equation (6) and considered the replacement rate of RA, as shown in Figure 6 and Equations (7) and (8), and summarized in.

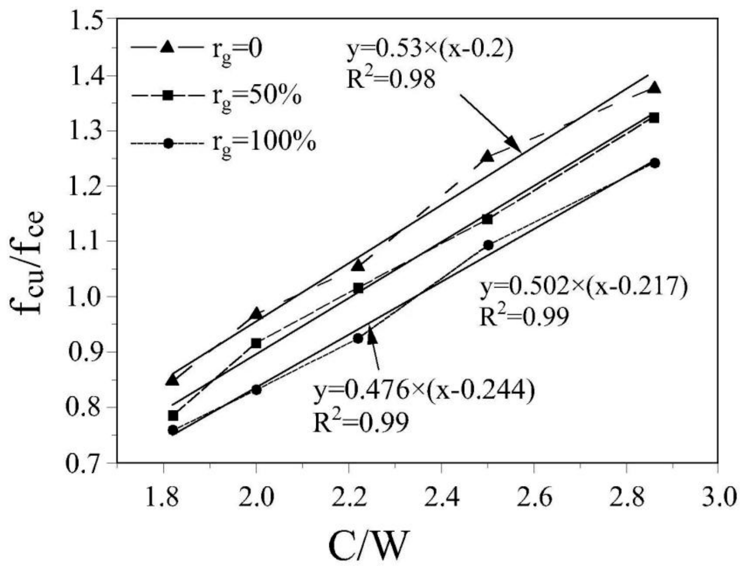


**Figure 6.** Fitting of the water-cement ratio of steel fiber recycled concrete [61].

Hua et al. [65] developed a sketch map of the mixed ratio design of RAC based on Abram's' law, Lyse's' law, and Molinari's law [66,67]. The water-cement ratio of RAC can be determined by selecting an appropriate mix ratio for different workability or strength values of RAC, as shown in Figure 7. Abram's law describes the relationship between the water-cement ratio ($C/W$) of concrete and the strength of concrete, as follows Equation (9). Lyse's law describes the relationship between the aggregate-cement ratio (A/C) and the water-cement ratio ($C/W$) (by weight) as follows Equation (10). Molinari's law describes the relationship between the aggregate-cement ratio and the cement content as follows Equation (11).

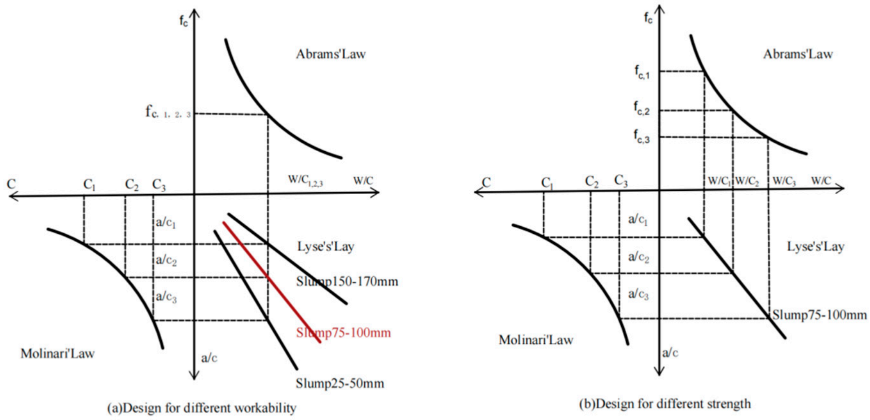


**Figure 7.** Design for different workability values and design for different strength values [65].

### *3.4. Unit Water Consumption*

Compared with NA, RA has high porosity and high water-absorption [68,69]. Many factors affect concrete water absorption [70]; therefore, the performance of RAC is lower than that of NAC for the same mix ratio [71–75]. RA can be modified on the surface or can be soaked to reduce the water absorption [76]. The pre-saturation method and water compensation method can be used when mixing RAC [67]. In the latter method, to improve the strength of RAC, water is added twice when pouring RAC [77,78]. However, these methods only change the water absorption of RA, and do not provide a calculation method of the unit water consumption of RAC.

Based on the replacement rate and quality of RA, Guo et al. proposed a calculation formula for the absolute water consumption of RAC [79–86]. Three different qualities of RA were obtained by physical strengthening, as shown in Tables 3 and 4 and Figure 8. Studies have shown that the absolute water consumption of RAC has a good linear relationship with the RA quality (Equation (12)), and the absolute water consumption decreases with an improvement in the RA quality [87]. The relationship between $\omega_a$, $\rho_0$, and $Q_e$ is: $\omega_a > \rho_0 > Q_e$, thus the formula of water consumption of RAC is as follows (Equation (13)).

**Table 3.** Basic performance indices of recycled coarse aggregate.

| Category | SC-RA | OP-RA | DP-RA |
|---|---|---|---|
| Particle size distribution | Continuous grain size | Continuous grain size | Continuous grain size |
| Elongated and flaky particle/% | 6 | 4 | 1 |
| Apparent density/(g/cm$^3$) | 2.432 | 2.468 | 2.475 |
| Packing density/(g/cm$^3$) | 1.355 | 1.389 | 1.407 |
| Porosity/% | 44 | 44 | 43 |
| Content ofimpurtities/% | 0.8 | 0.5 | 0.1 |
| Content of harmful substances | Qualified | Qualified | Qualified |
| Alkali aggregate reaction | Qualified | Qualified | Qualified |
| Content of fine powder/% | 1.9 | 1.1 | 0.8 |
| Content of clay particles/% | 0.6 | 0.2 | 0.1 |

**Table 3.** *Cont.*

| Category | SC-RA | OP-RA | DP-RA |
|---|---|---|---|
| Water absorption/% | 3.7 | 2.3 | 1.7 |
| Crushing index/% | 18 | 15 | 9 |
| Soundness/% | 8.9 | 5.7 | 3.1 |
| Aggregate type | Class II | Class II | Class I |

Notes: 1. SC-RA denotes simple crushing recycled aggregate. 2. The OP-RA denotes physically strengthened (once) recycled aggregate. 3. The DP-RA denotes physically-strengthened recycled aggregate. 4. Class I-II denotes RA is classified as first or second level.

**Table 4.** Results of linear regression of the impact factor of the recycled aggregate and quality.

| Category | Linear Regression Equation | Correlation of Determination ($R^2$) |
|---|---|---|
| $\beta_g$-$\rho_0$ | $\beta_g = -0.238\rho_0 + 604.5$ | 0.949 |
| $\beta_g$-$\omega_a$ | $\beta_g = 540.9\omega_a + 6.635$ | 0.999 |
| $\beta_g$-$Q_e$ | $\beta_g = 111.6Q_e + 4.900$ | 0.696 |

Notes: 1. The $\rho_0$ is the apparent density of the recycled coarse aggregate (kg·m$^{-3}$); 2. The $\omega_a$ is the water absorption of the recycled coarse aggregate in decimals; 3. The $Q_e$ is the crushing index of the recycled coarse aggregate in decimals. 4. $R^2$ is the coefficient of determination and not the correlation coefficient.


**Figure 8.** Three kinds of RA with different qualities; (**a**) SC-RA; (**b**) OP-RA; (**c**) DP-RA.

In China, the unit water consumption of ordinary concrete is determined using tables, or by the following Equation (14) [83]. Gao et al. [62] obtained a linear relationship between the slump level and unit water consumption of RAC using orthogonal experiments, as shown in Figure 9. The replacement rate and water absorption rate of RAC in Equations (15) and (16) were used to fit the curve.

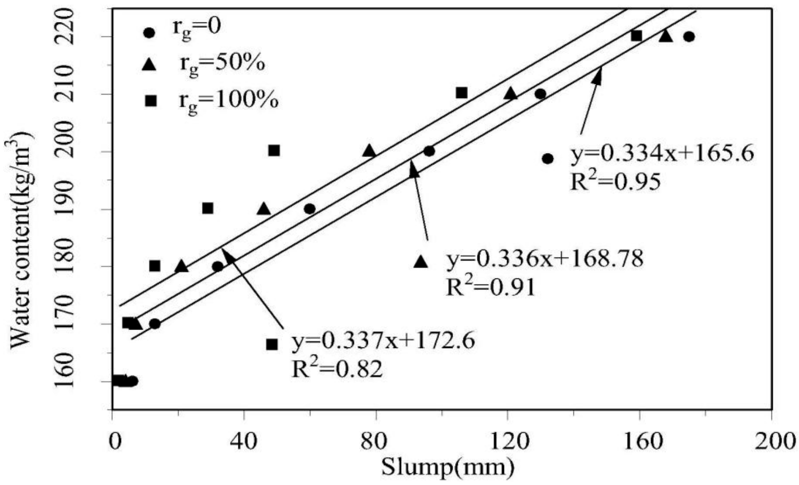


**Figure 9.** Relationship between the slump level and the unit water consumption of SF RAC [61].

Wang Min et al. mixed RA with brick slag [84–86] and developed Equation (15). A water absorption test was conducted with a recycled brick slag aggregate (RBSA) [88,89]. The relationship between the incremental coefficient and time of the RBSA is shown in Figure 10. The relationship is described in Equations (16)–(22). Zhang-Deng [65] proposed Equation (16) to calculate the additional water consumption of RAC, which is used in the technical specification for recycled concrete structures (solicitation draft). Equation (17) was developed by referring to Zhang [90,91]. Equation (23) was proposed (28) to calculate the additional water in the mixture ratio design of brick slag RAC [91]. Equations (18) and (22) are substituted into Equation (17) to obtain Equation (23), describing the relationship between the additional water content and time to design of the mixture ratio of recycled concrete containing RBSA.

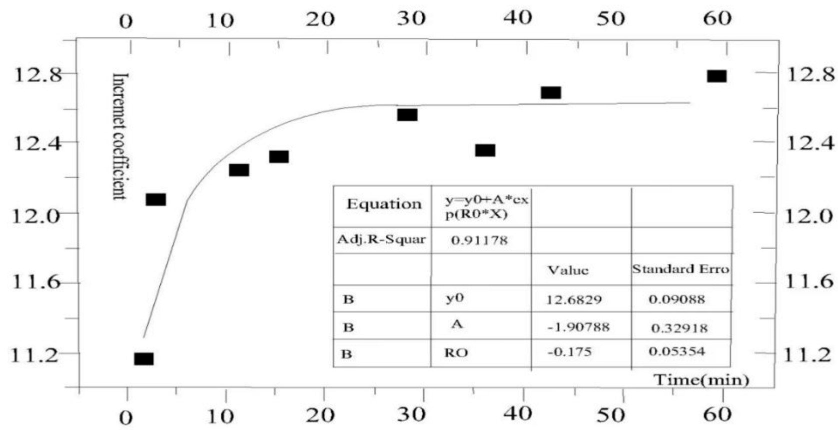


**Figure 10.** Relationship between the incremental coefficient k and time for different water contents in BSA in brick slag aggregate [90].

### 3.5. Cement

Ordinary Portland cement (OPC) and sulphoaluminate cement (CSA) are two commonly used types of cement; the oxide and chemical compositions of cement are shown in Table 5. The product is created by the hydro-hardening of CSA cement, whereas the hydro-hardening product of Portland cement is a calcium silicate compound. CSA cement has a higher content of tricalcium aluminate ($C_3A$) and $Ca_4Al_6O_{12}SO_4$ than OPC, resulting in a higher early strength of the CSA cement compared to OPC. Hua et al. [65] used OPC cement and CSA cement to investigate the lead content of lead-contaminated RA (the average lead content measured by the wet extraction method was 25.5 mg/L) and lead-contaminated RBSA (the average lead content measured by the wet extraction method was 9.16 mg/L), respectively [92,93]. The California code [94–104] defines hazardous materials as having a lead concentration exceeding 1 mg/L (wet extraction). It was found that the lead concentration of RAC and recycled brick slag concrete (RBSC) was less than 1mg/L (wet extraction), and the RA and RBSA containing OPC was better than those containing CSA because OPC cement is more alkaline than CSA [65].

**Table 5.** Oxide and chemical compositions of cement (%).

| | | | | | | | | |
|---|---|---|---|---|---|---|---|---|
| Oxide Composition (%) | PortlandCSA | CaO | $SiO_2$ | $Al_2O_3$ | $Fe_2O_3$ | MgO | $SO_3$ | $TiO_2$ |
| | | 62.96<br>40.00 | 20.96<br>5.55 | 4.54<br>37.50 | 3.48<br>1.50 | 2.91<br>1.75 | 2.77<br>10.00 | -<br>1.25 |
| Chemical Composition (%) | PortlandCSA | $C_3S$ | $C_2S$ | $C_3A$ | $C_4AF$ | Gypsum | $Ca_4Al_6O_{12}SO_4$ | |
| | | 53.71<br>0.42 | 19.58<br>12.59 | 6.14<br>10.64 | 10.59<br>- | 0.78<br>1.07 | -<br>73.37 | |

Cement dosages can be determined using the calculation method of the $C/W$ ratio described in Section 3.2. The unit water consumption is obtained using the calculation method of unit water consumption presented in Section 3.3. Alternatively, the nomogram of the general mix design [65] can be used to determine the cement dosage, as shown in Figure 8.

### 3.6. Sand Ratio

The surface of RA is covered by a layer of mortar, unlike NA, and the presence of the mortar reduces the performance of the RAC [105,106]. Crushing of low-strength concrete reduces the amount of mortar adhering to the RA surface, but crushing of high-strength concrete increases the bonding strength between the mortal and the RA [107]. Therefore, researchers have proposed different calculation methods to determine the ratio of recycled concrete and sand.

Guo et al. [64] used the calculation method of NAC to determine the sand-to-concrete ratio of RAC when physical and chemical strengthening methods were applied. The sand-to-concrete ratio rate of NAC ($\beta_{sN}$) should be determined based on the standard JGJ55-2011 [108], the technical parameters of the aggregate, the concrete mixing performance, and the construction requirements, as shown in Equation (24–25).

Fathifazl used the equivalent mortar volume (EMV) method, and considered the mortar adhered to the RA versus total mortar content of RAC to determine the parameters of normally vibrated concrete (NVC) [109].

Gao et al. considered the cement mortar covering the outer layer of the RA and the particles inside the cement mortar as one unit. The objective was to fill the gap between concrete and the coarse aggregate with fine aggregate. The following Equations (26)–(29) were established to calculate the sand ratio of the SF recycled concrete [62], as summarized in Table 6.

### 3.7. Annexing Agent

Fly ash, SPs, water-reducing agents, and AGs are the primary additives of RAC. Fly ash is artificial ash with a smooth and spherical particle that can fill the pore of cement paste, reducing the water requirements; the pozzolanic reaction of the fly ash cement paste is the chemical reaction between reactive silica or Alumina in the fly ash particles and calcium hydroxide ($Ca(OH)_2$-CH), formed from cement hydration. Fly ash can reduce the porosity of the concrete and improve the bonding capacity of the aggregate and cement mortar [110–112]. SP has high activity and high filling capacity and is widely used in various kinds of concrete admixtures to improve the workability and bonding performance of the concrete. SP has the ability to resist alkali-aggregate reaction and sulfate, and has low permeability [48]. RA has a high water-absorption capacity; thus, additional water has to be added to improve the workability. However, an increase in the water content may affect the mechanical properties of RAC. Therefore, water-reducing agents are utilized to reduce the water content and improve the workability of RAC; these agents do not adversely affect the RAC [113,114]. Accelerating agents have been used in shotcrete; however, there is a lack of research on spraying recycled concrete or SF recycled concrete using shotcrete. A compatibility test must be performed when an accelerating agent, fly ash, and a water reducer are used simultaneously. The amount of additives in RAC have not been investigated in depth. Generally, a conventional amount of ordinary concrete is used: fly ash or SP typically comprises 10% of the cement amount, and the dosage of a highly effective water-reducing agent is generally 1.5% of the weight cementious material.

**Table 6.** Equation of mixture ratio of RAC.

| Composition Material | Equation | | Symbol Description | Ref. |
|---|---|---|---|---|
| Amount of RA | $\frac{m_c}{p_c} + \frac{m_f}{p_f} + \frac{m_g}{p_g} + \frac{m_s}{p_s} + \frac{m_w}{m_w} + 0.001\alpha \ = 1$ | (1) | $p_c$: cement density (kg/m$^3$), $p_f$: mineral admixtures (SF and fly ash, SP, etc.) density (kg/m$^3$), $p_g$: (RA and NA) aggregate of the apparent density (kg/m$^3$), $p_s$: fine aggregate of apparent density (kg/m$^3$), $p_W$: water density is 1000 kg/m$^3$, $\alpha$: percentage of the air content of concrete, $\alpha$ desirable 1 without using air-entraining agent for RAC, $\alpha$ preferable 2 without air-entraining agent for SF reinforced concrete, $m_c$: cement dosage (kg/m$^3$), $m_f$: mineral admixture dosage (kg/m$^3$), $m_s$: sand dosage (kg/m$^3$), $m_W$: unit water consumption (kg/m$^3$). | (1) [52] |
| Steel fiber content | $f_{ftm}/f_{tm} = \alpha_f \lambda_f^2 + B_f$ | (2) | $f_{ftm}$, $f_m$: the flexural strength of the SF RAC and the RAC with the same mix ratio respectively, $v_f$: the volume rate of the SF, $l_f/d_f$: the slenderness ratio of the SF, $f_t$: the splitting strength of the concrete matrix, $R$: the volume ratio of the SF, $f_r$: the design value of the tensile strength of the SF, $f_{ce}$: the 28-day splitting strength of the cement. | (2–3) [61,62] (4) [63] |
| | $\lambda_f = v_f l_f / d_f$ | (3) | | |
| | $f_t = 6.66 \times 10^{-5}\ R\ f_r + 3.46 \times 10^{-2}\ f_{ce} \frac{c}{w}$ | (4) | | |
| Water/cement ratio | $f_{cu,0} = f_{ce}(C/W - \alpha_b)$ | (5) | $f_{cu,0}$: denotes the design compressive strength (MPa) of the concrete or RA, $f_{ce}$: is the 28-day compressive strength(Mpa) of the cement, $C/W$: the water/cement | (5–6) [64] (7–11) [66,67] |
| | $f_{Rg} = A\ f_{ce}\left[C/\left(W\ + m_{Rg} w_a\right) + B\ \right]$ | (6) | | |
| | $\alpha_a = 0.53\ \left(1\ - 0.1 r_g\right)$ | (7) | | |
| | $\alpha_b = 0.2\ \left(1\ + 0.2 r_g\right)$ | (8) | ratio, $\alpha_a$: cement strength conversion coefficient, $\alpha_b$: (virtual water-cement ratio) are the regression coefficients for data fitting, $f_{R_g} = f_{cu,0}$, $A = \alpha_a$, and $B = \alpha_b$, $w$: the water consumption of ordinary concrete, $m_{R_g}$: the dosage of RCA (kg·m$^{-3}$), $w_a$: the water absorption rate of RCA, which is expressed by decimals, $k_1$ and $k_2$ are constants that depended on the material, $a/c$: the ratio of aggregate to cement, $k_3$ and $k_4$ are constants that depend on the material used, C: the cement content, $k_5$ and $k_6$ are constants that depend on the material. | |
| | $f_c' = \frac{k_1}{k_2^{w/c}}$ | (9) | | |
| | $(a/c) = k_3(w/c) + k_4$ | (10) | | |
| | $C\ = \frac{1000}{k_5(a/c) + k_6}$ | (11) | | |

**Table 6.** *Cont.*

| Composition Material | Equation | Symbol Description | Ref. |
|---|---|---|---|
| Unit water consumption | $W_{Rg} = W + \beta_g \lambda_g$ (12)<br>$W_{Rg} = W + (540.9 w_a + 6.635)\lambda_g$ (13)<br>$m_w = 3.33 \times (0.1 \times T_0 + K)$ (14)<br>$m_w = 3.33 \times (0.1 \times T_0 + k_g)$ (15)<br>$k_g = k\left[1 + (w_{ra} - w_{na}) \times r_g\right]$ (16)<br>$\triangle W = \mu \triangle W_z + (1 - \mu) \triangle W_c$ (17)<br>$\triangle W_c = \begin{cases} \left(2.00569 - 0.61793\, e^{-0.2048t}\right)\% m_R & 0 < t < 60 \text{ min} \\ \left(1.99318 + 1.1023\, e^{-4}t\right)\% m_R & 60 \text{ min} < t < 24 \text{ h} \\ 2.15\% m_R & t > 24 \text{ h} \end{cases}$ (18)<br>$\triangle W = m_g[(S_R - w_R) - (S_0 - w_0)]$ (19)<br>$k = (S_R - w_R) - (S_0 - w_0)$ (20) | $W_{R_g}$: the total water consumption of RAC, $\beta_g$: the influence coefficient of the absolute water consumption of RAC that has a linear relationship with the performance indices of RAC (Table 4), $m_w$: the unit water consumption ($\text{kg/m}^3$), $T$: the slump level of ordinary concrete (mm), $K$: a constant, which is determined by the type and the maximum particle size of the coarse aggregate, $T_0$ the required slump level of RAC, $k_g$: the coefficient related to the type and particle size of RA, $w_{ra}$: the water absorption rate of RA, $w_{na}$: the water absorption rate of NA. | (12–13) [79]<br>(14) [83]<br>(15–16) [62]<br>(17–24) [92] |
| | $k = \begin{cases} \left(12.683 - 1.908 e^{-0.175t}\right)\% & 0 < t < 60 \text{ min} \\ (13.415 + 0.0005t)\% & 60 \text{ min} < t < 24 \text{ h} \\ 14.14\% & t > 24 \text{ h} \end{cases}$ (21)<br>$\triangle W_z = \begin{cases} \left(12.683 - 1.908 e^{-0.175t}\right)\% m_R & 0 < t < 60 \text{ min} \\ (13.415 + 0.0005t)\% m_R & 60 \text{ min} < t < 24 \text{ h} \\ 14.14\% m_R & t > 24 \text{ h} \end{cases}$ (22)<br>$\triangle W_c = \begin{cases} \left[2 + 10.683\mu - e^{-0.2t}(1.278\mu + 0.62)\right]\% m_R & 0 < t < 60 \text{ min} \\ [\mu(11.425 + 0.00039t) + 1.99 + 0.0001t]\% m_R & 60 \text{ min} < t < 24 \text{ h} \\ (2.15 + 11.99\mu)\% m_R & t > 24 \text{ h} \end{cases}$ (23) | | |
| Cement | $C/W$ (24) | | |
| Sand ratio | $\beta_s = \beta_{sN} - \frac{m_{RA} - m_{ACSN}}{m_{RA}}\%$ (25)<br>$V_s = \gamma \times \left(V_{na} \times P_{na} + V_{ra} \times P_{ra} + V_f\right)$ (26)<br>$V_c + V_w + V_s + V_{na} + V_{ra} + V_f + +\alpha = 1$ (27) | $m_{RA}$: the quality of RA in the drying state, $m_{ACSN}$: the quality of RA completely stripped by a freeze-thaw cycle (Figure 3), $\beta_{sN}$: the sand rate of RA after stripping the | (25) [109]<br>(26–29) [62] |
| | $r_g = \frac{m_{ra}}{m_{ra} + m_{na}} = \frac{\rho_{ra} \times V_{ra}}{\rho_{ra} \times V_{ra} + \rho_{na} \times V_{na}} \Rightarrow \frac{V_{na}}{V_{ra}} = \frac{\left(1 - r_g\right) \times \rho_{ra}}{r_g \times \rho_{na}}$ (28)<br>$\beta_g = \frac{m_s}{m_s + m_{na} + m_{ra}} = \frac{\rho_{ra} \quad V_s}{\rho_s V_s + \rho_{na} V_{na} + \rho_{ra} V_{ra}}$ (29) | cement mortar from the NAC and represents the sand ratio of RAC. $\gamma$: the coefficient of sand ratio surplus, which is the ratio of fine aggregate sand in RAC to the pore volume of the RA and SF. $V_s$, $V_m$, $V_{ra}$ and $V_f$ represent the volumes of sand, NA, RA, and SF, respectively. $P_{na}$ and $P_{ra}$ represent the porosity of NA and RA respectively. $V_c$ and $V_w$ represent the volume of cement and water in RAC respectively,represents the air content of RAC. $m_s$, $m_{ra}$, and $m_{na}$ represent the quality of sand, NA, and RA, respectively. $\rho_s$, $\rho_m$, and $\rho_{na}$ represent the density of sand, NA, and RA, respectively. | |

## 4. Mechanical Properties of RAC

In this section, we summarize the factors affecting the compressive properties, flexural properties, shear properties, and durability of RAC, and focus on the methods of improving the mechanical properties of RAC.

### 4.1. Compressive Performance

The compressive property is the most crucial mechanical property of RAC, since it affects the bending and shear properties and the durability of RAC. The compressive strength of RAC decreases with an increase in the replacement rate of RA [115–120]. A high replacement rate of RA has been the objective of numerous studies, and the improving of the quality of the RA itself is imperative to achieve this. Physical and chemical methods to improve the quality of RA were described in Section 3.1.1, and will not be repeated here.

The water-cement ratio is a key factor affecting the compressive strength of RAC. The compressive strength of RAC decreases with an increase in the water-cement ratio, and the same applies to ordinary concrete [121]. Cement mortar is bonded to the surface of RA, and the porosity and water-absorption capacity are high. The water consumption of RAC is higher than that of ordinary concrete to achieve the same workability. In general, the influence of this adverse factor is reduced by adding a water-reducing agent and adding water in two stages [83,84].

The addition of SF can improve the compressive performance of RAC [120], and improve the distribution of micro-cracks. The mechanical reinforcement mechanism of SF is detailed in Sections 3.2.1 and 3.2.2. Numerous domestic and international studies on SF recycled concrete have shown that the compression behavior of SF recycled concrete is similar to that of SF ordinary concrete. SFs significantly improve the mechanical properties of RAC and change the fracture process and toughness of RAC [122–124]. SFs prevent or reduce the development of micro-cracks inherent in RAC [17]. As partial substitutes of cement gel materials, fly ash and SP substantially improve the compressive performance of RAC [115–117]. The microscopic analysis of RAC with SP described in Section 5 also confirms this result.

### 4.2. Bending and Shear Properties

The flexural and shear properties of RAC decrease with an increase in the replacement rate of RA [122–129]. At the replacement rates of RA of 25%, 50%, and 100% the bending strength of RAC was 6%, 13%, and 26% lower, respectively, than that of ordinary concrete with the same mix ratio, and the splitting shear strength of RAC was 6%, 10%, and 40% lower, respectively, than that of ordinary concrete with the same mix ratio [123]. Zhang et al. [130] found that SF significantly improved the bending performance and shear performance of RAC. The SF did not significantly enhance the bending performance of RAC when the volume ratio of the SF was less than 0.5%. However, when the volume ratio of the SF in RAC increased from 0.5% to 1%, the bending performance of RAC increased significantly. When the volume ratio of SF was > 1%, the bending performance of RA decreased significantly with an increase in the volume ratio. An increase in the volume ratio of SF from 0% to 2% resulted in an increase in the split shear strength of RAC of 84%.

## 5. The Durability of RAC

The durability of RAC has attracted much attention. A review of studies on chloride penetration, sulfate erosion, freeze-thawing cycles, and high temperature indicates that the durability of the RAC is attributed to the high porosity and high water-absorption capacity.

(1) Chloride Permeability: The higher the porosity, the stronger the chloride ion permeability is, and the lower the chloride ion resistance of RAC is [125–128]. However, when fly ash and SP are added to RAC, they fill the pores of RAC and decrease the chloride ion permeability of RAC [129–131]. (2) Sulfate Attack: The replacement rate of RA has the largest influence on the sulfate erosion resistance of RAC [132–138]. However, studies have found that different replacement rates of RA (50%, 70%, 100%) have a negligible

influence on the sulfate penetration rate of RAC [134]. Volcanic ash refines the pores of RAC, improves the interface bonding ability, and significantly improves the sulfate resistance of RAC [134–136]. (3) Freezing and Thawing: The freeze-thawing state of RAC is divided into two processes: first, the performance and saturation of the constituent materials of RAC determine the freezing behavior of the matrix; second, the porosity of the RA determines the freezing behavior of the aggregate [137], which has adverse effects on the RAC. Researchers found that the dynamic modulus values of NAC and RAC did not change after 300 freeze-thaw cycles when a low water-binder ratio (W/C = 0.35) was used, and gas was added: the amount of RA had little impact on the durability [138,139]. However, the quality, strength, and porosity of RA were not considered. These parameters are worthy of further study to determine the RAC performance in the freeze-thaw cycle tests. (4) High-Temperature Exposure: The thermal expansion coefficient of a concrete structure is different for high-temperature and low-temperature cooling, affecting the durability of concrete in terms of spalling and volume changes. Research has shown that for the same particle size of RCA covered in cement mortar, the thermal expansion coefficient of the RA and mortar were similar, unlike that of NAC. Therefore, the resistance of the RAC to high temperatures and degradation is better than that of normal NAC [140–162].

## 6. Microanalysis of RAC with an Optimized Mix Ratio

The performance of RA is worse than that of NA, and the strength of RAC prepared with a mixture ratio of ordinary concrete is 5%–24% lower [138–142]. The two-stage water addition method [77,78], EMV method [108], and the addition of SP [117–120,150–154] were used to improve the mechanical properties of RAC, as summarized in Section 3. In this section, we explain the principle of micro-mechanical properties of RAC using an example of the micro-analysis of self-compacting RAC (SRAC), as shown in Figure 11.

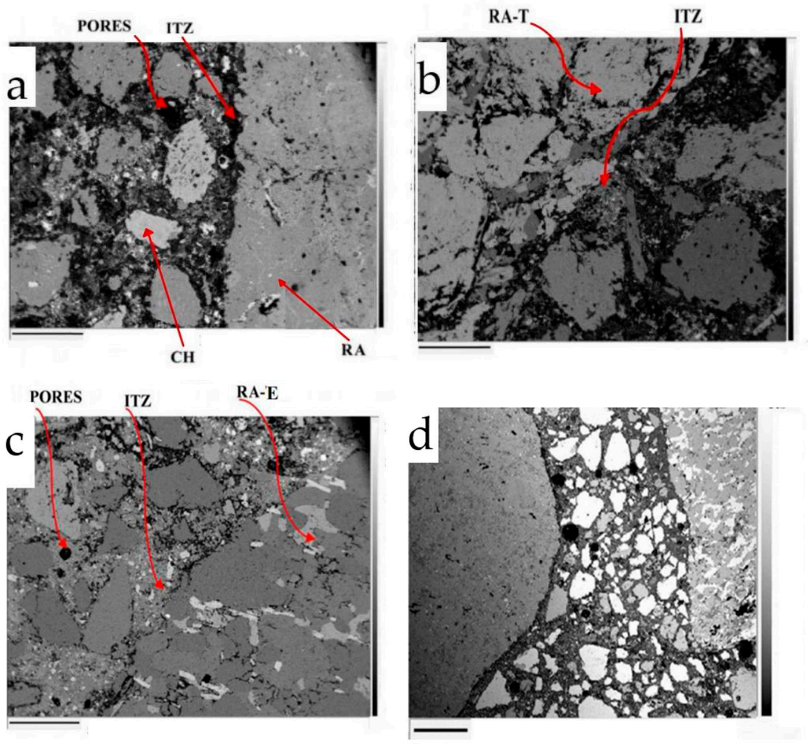


**Figure 11.** Micro-analysis of SRAC [112]. ((**a**) Traditional method to prepare SRAC. (**b**) Two-stage water addition method to prepare SRAC. (**c**) Equivalent mortar volume method to prepare SRAC. (**d**) Addition of silica powder to prepare SRAC. CH stands for calcium hydroxide; ITZ stands for interfacial transition zone between aggregate and cement mortar; RA-T stands for two-stage water addition method of SRAC; RA-E stands for equivalent mortar volume method of SRAC; BSE stands for Backscatter Secondary Electron Image Analysis).

Figure 11a shows that the bonding performance between the aggregate and cement mortar is poor; the interface transition zone has several micro-cracks, and the concrete has many pores with a large pore diameter when SRAC is prepared using the common concrete mix method. However, when the two-stage water addition method is used to prepare the SRAC, the matrix performance of the concrete is well improved, the porosity is reduced, the bonding strength between the SRCA and cement mortar is increased, and there are fewer micro-cracks, as shown in Figure 11b. The EMV method was used to prepare SRAC. Compared with Figure 11a,c, the pore diameter in Figure 11c is smaller, the bonding strength between RA and cement mortar is higher, and the interfacial zone is compact and not loose. Compared with Figure 11b, the composite material distribution of the SRAC body is more uniform and compact in Figure 11c. Figure 11d shows the presence of silica in the interfacial transition zone after the addition of SP to the SRAC. The silica-reactive energy reacts with the Portland cement to form an additional and improved binder similar to calcium silicate hydrate (CS-H) crystals.

The microscopic images and analysis demonstrate the mixed-ratio design method reviewed in Section 3, and the addition of SP or other materials significantly improved the mechanical properties of RAC. However, many methods exist to design the mixture ratio of RAC, and there is no unified worldwide standard.

## 7. Conclusions

In this paper, the technical route, composition materials, properties, and design methods of the mix proportion of RAC were reviewed. The mechanical properties, durability, and microanalysis of RAC are also discussed. It is of great significance for sustainable development in civil engineering and architecture to prepare concrete with RA instead of NA. The quality of RA is improved by the physical and chemical treatment, and the design parameters of the mix ratio are optimized. The mechanical properties and durability of recycled concrete are improved by adding SP, SF, and other auxiliary materials. We provide the following suggestions to promote the extensive and scientific application of recycled concrete in the field of architecture in the future; this paper proposes the following suggestions:

1. Research is lacking on the use of RA for shotcrete, which is widely used in tunnel construction, slope support, and other fields. It is important to investigate the mixture design, mechanical properties, and durability of shotcrete recycled concrete or shotcrete SF recycled concrete.
2. There is no unified understanding of the replacement rate of RA with different qualities. It is necessary to define the upper limit of the replacement rate of RA with different qualities and the effect of enhancing the mechanical properties of auxiliary materials, so as to promote the extensive application of RAC. In order to reduce the cost of using them in various chemical or physical treatments, the effective water in the recipe must be established and the quality of RA aggregates should be checked more frequently compared to NA.
3. Many methods exist for the mix design of RAC, and each has its advantages. It is necessary to reach a consensus to understand the advantages of different methods and standardize the mix design of RAC.
4. It is necessary to determine how to handle the treatment and reuse of harmful RA and building material to prevent exposure to harmful substances after break-down and adverse impacts on the environment.
5. Research is also lacking on the alkali-aggregate reaction of RAC, which occurs when the alkaline substance in the concrete reacts with the active ingredient, causing expansion of material or water absorption. Internal cracking occurs due to expansion stress. Commonly, the concrete-alkali-aggregate reaction causes cracking of the coarse aggregate, which is more destructive than the damage to the cement mortar colloid or the over-bond layer between the cement mortar and aggregate. However, RA is generated by the demolition of concrete structures, and the alkalinity is neutralized. If an alkali-aggregate reaction occurs, damage will occur. Therefore, it can be assumed

that RAC is relatively resistant to the alkali-aggregate reaction, although this has not been confirmed by studies to date.

**Author Contributions:** Conceptualization, C.L. and Y.W.; methodology, G.Z.; software, H.L.; validation, C.M., X.G. and J.S.; formal analysis, X.G.; investigation, Y.W.; resources, X.G..; data curation, G.Z.; writing—original draft preparation, X.G.; writing—review and editing, C.L.; visualization, H.L.; supervision, J.S.; project administration, J.L.; funding acquisition, J.L. All authors have read and agreed to the published version of the manuscript.

**Funding:** This research was funded by [Special Fund for Campus Nature Fund of Qingdao University of Technology of China] grant number [No. 2021C005] and National Natural Science Foundation of China [No. 51978066].

**Institutional Review Board Statement:** Not applicable.

**Informed Consent Statement:** Not applicable.

**Data Availability Statement:** All data, models, and code generated or used during the study appear in the submitted article.

**Conflicts of Interest:** The authors declare that they have no conflict of interest.

## References

1. Marie, I.; Quiasrawi, H. Closed-loop recycling of recycled concrete aggregates. *J. Clean. Prod.* **2012**, *37*, 243–248. [CrossRef]
2. Radonjanin, V.; Malešev, M.; Marinković, S.; Al Malty, A.E.S. Green recycled aggregate concrete. *Constr. Build. Mater.* **2013**, *47*, 1503–1511. [CrossRef]
3. Zhang, W.; Ingham, J.M. Using Recycled Concrete Aggregates in New Zealand Ready-Mix Concrete Production. *J. Mater. Civ. Eng.* **2010**, *22*, 443–450. [CrossRef]
4. Lim, W.F.; Chew, K.C.; Zayed, T.; Lee, Y.P.K.; Low, G.L.; Ting, S.K.; Ho, N.Y. Efficient Utilization of Recycled Concrete Aggregate in Structural Concrete. *J. Mater. Civ. Eng.* **2013**, *25*, 318–327.
5. De Juan, M.S.; Gutiérrez, P.A. Study on the influence of attached mortar content on the properties of recycled concrete aggregate. *Constr. Build. Mater.* **2009**, *23*, 872–877. [CrossRef]
6. Duan, Z.H.; Poon, C.S. Properties of recycled aggregate concrete made with recycled aggregates with different amounts of old adhered mortars. *Mater. Des.* **2014**, *58*, 19–29. [CrossRef]
7. Tam, V.W.Y.; Gao, X.F.; Tam, C.M.; Chan, C.H. New approach in measuring water absorption of recycled aggregates. *Constr. Build. Mater.* **2008**, *22*, 364–369. [CrossRef]
8. Medina, C.; Zhu, W.; Howind, T.; Sánchez De Rojas, M.I.; Frías, M. Influence of mixed recycled aggregate on the physical—Mechanical properties of recycled concrete. *J. Clean. Prod.* **2014**, *68*, 216–225. [CrossRef]
9. Li, J.S.; Xiao, H.N.; Zhou, Y. Influence of coating recycled aggregate surface with pozzolanic powder on properties of recycled aggregate concrete. *Constr. Build. Mater.* **2009**, *23*, 1287–1291. [CrossRef]
10. Han, S.; Li, Q. Effect of physical and chemical strengthening on shrinkage performance of recycled concrete. *Compr. Util. Fly Ash* **2016**, *2*, 3–7.
11. Wang, L.; Gu, Y. Study on the Influence of Nanometer Strengthening technology on the durability of recycled concrete. *Concrete* **2014**, *7*, 48–51.
12. Shima, H.; Tateyashiki, H.; Matsuhashi, R.; Yoshida, Y. An advanced concrete recyc1ing technology and its applicability assessment through input-output analysis. *J. Adv. Concr. Technol.* **2005**, *3*, 53–67. [CrossRef]
13. Sui, Y.W.; Mueller, A. Development of thermo-mechanical treatment for recycling of used concrete. *Mater. Struct.* **2012**, *45*, 1487–1495. [CrossRef]
14. Ryu, J. Improvement on strength and impermeability of recycled concrete made with crushed concrete coarse aggregate. *J. Mater. Sci. Lett.* **2002**, *21*, 1565–1567. [CrossRef]
15. Zhan, B.; Xuan, D.; Poon, C.S. Enhancement of recycled aggregate properties by accelerated $CO_2$ curing coupled with lime water soaking process. *Cem. Concr. Compos.* **2018**, *89*, 230–237. [CrossRef]
16. Ismail, S.; Ramli, M. Engineering properties of treated recycled concrete aggregate (RCA) for structural applications. *Constr. Build. Mater.* **2013**, *44*, 464–476. [CrossRef]
17. Zaetang, Y.; Sata, V.; Wongsa, A.; Chindaprasirt, P. Properties of pervious concrete containing recycled concrete block aggregate and recycled concrete aggregate. *Constr. Build. Mater.* **2016**, *111*, 15–21. [CrossRef]
18. Carneiro, J.A.; Lima, P.R.L.; Leite, M.B.; Toledo Filho, R.D. Compressive stress–strain behavior of steel fiber reinforced-recycled aggregate concrete. *Cem. Concr. Compos.* **2014**, *46*, 65–72. [CrossRef]
19. Senaratne, S.; Gerace, D.; Mirza, O.; Tam, V.W.; Kang, W.H. The costs and benefits of combining recycled aggregate with steel fibres as a sustainable, structural material. *J. Clean. Prod.* **2016**, *112*, 2318–2327. [CrossRef]

20. Yang, H.; Ding, Y. Comparative analysis of physical and mechanical properties of different kinds of fiber reinforced concrete. *Constr. Technol.* **2018**, *20*, 6–9.
21. Qiao, H.; Li, J. Effect of fiber mixing method on frost resistance of concrete. *Silic. Notif.* **2019**, *17*, 495–500.
22. Somna, R.; Jaturapitakkul, C.; Chalee, W.; Rattanachu, P. Effect of the Water to Binder Ratio and Ground Fly Ash on Properties of Recycled Aggregate Concrete. *J. Mater. Civ. Eng.* **2012**, *24*, 16–22. [CrossRef]
23. Meyer, C. The greening of the concrete industry. *Cem. Concr. Compos.* **2009**, *31*, 601–605. [CrossRef]
24. Liang, Y.; Ye, Z.; Vernerey, F.; Xi, Y. Development of Processing Methods to Improve Strength of Concrete with 100% Recycled Coarse Aggregate. *J. Mater. Civ. Eng.* **2015**, *27*, 04014163. [CrossRef]
25. Tam, C.T.; Akbarnezhad, A.; Zhang, M.H.; Ong, K.C.G. Effects of the Parent Concrete Properties and Crushing Procedure on the Properties of Coarse Recycled Concrete Aggregates. *J. Mater. Civ. Eng.* **2013**, *25*, 1795–1802.
26. Butler, L.; West, J.S.; Tighe, S.L. Effect of recycled concrete coarse aggregate from multiple sources on the hardened properties of concrete with equivalent compressive strength. *Constr. Build. Mater.* **2013**, *47*, 1292–1301. [CrossRef]
27. Limbachiya, M.; Meddah, M.S.; Ouchagour, Y. Use of recycled concrete aggregate in fly-ash concrete. *Constr. Build. Mater.* **2012**, *27*, 439–449. [CrossRef]
28. Mas, B.; Cladera, A.; Olmo, T.D.; Pitarch, F. Influence of the amount of mixed recycled aggregates on the properties of concrete for non-structural use. *Constr. Build. Mater.* **2012**, *27*, 612–622. [CrossRef]
29. Tam, V.W.Y.; Tam, C.M.; Wang, Y. Optimization on proportion for recycled aggregate in concrete using two-stage mixing approach. *Constr. Build. Mater.* **2007**, *21*, 1928–1939. [CrossRef]
30. *GB14684-2011*; Building Sand. China Standard Press: Beijing, China, 2011.
31. Larsen, R.J.; Marx, M.L. *An Introduction to Mathematical Statistics and Its Application*, 2nd ed.; Prentice-Hall: Vandy, NJ, USA, 1986.
32. Pepe, M.; Toledo Filho, R.D.; Koenders, E.A.B.; Martinelli, E. A novel mix design methodology for Recycled Aggregate Concrete. *Constr. Build. Mater.* **2016**, *122*, 362–372. [CrossRef]
33. Zhang, L. *Mix Design and Performance Calculation Method of Steel Fiber Recycled Concrete*; Zhengzhou University: Zhengzhou, China, 2017; p. 20.
34. Khemissa, M.; Mahamedi, A. Cement and lime mixture stabilization of an expansive overconsolidated clay. *Appl. Clay Sci.* **2014**, *95*, 104–110. [CrossRef]
35. Lee, C.; Lee, K.; Choi, H.; Choi, H.P. Characteristics of thermally-enhanced bentonite grouts for geothermal heat exchanger in South Korea. *Sci. China-Technol. Sci.* **2010**, *53*, 123–128. [CrossRef]
36. Zhao, Z.G.; Qu, X.L.; Li, F.X.; Wei, J.X. Effects of steel slag and silica fume additions on compressive strength and thermal properties of lime-fly ash pastes. *Constr. Build. Mater.* **2018**, *183*, 439–450. [CrossRef]
37. Rajhans, P.; Panda, S.K.; Nayak, S. Sustainable self compacting concrete from C&D waste by improving the microstructures of concrete ITZ. *Constr. Build. Mater.* **2018**, *163*, 557–570.
38. Rajhans, P.; Panda, S.K.; Nayak, S. Sustainability on durability of self compacting concrete from C&D waste by improving porosity and hydrated compounds: A microstructural investigation. *Constr. Build. Mater.* **2018**, *174*, 559–575.
39. Gholampour, A.; Ozbakkaloglu, T. Time-dependent and long-term mechanical properties of concretes incorporating different grades of coarse recycled concrete aggregates. *Eng. Struct.* **2018**, *157*, 224–234. [CrossRef]
40. Shahidan, S.; Azmi, M.A.M.; Kupusamy, K.; Zuki, S.S.M.; Ali, N. Utilizing construction and demolition (C&D) waste as recycled aggregates (RA) in concrete. *Procedia Eng.* **2017**, *174*, 1028–1035.
41. Falek, K.; Aoudjane, K.; Kadri, E.H.; Kaoua, F. Influence of recycled aggregates on the mechanical and tribological behavior of concrete. *Energy Procedia* **2017**, *139*, 456–461. [CrossRef]
42. Kabir, S.; Al-Shayeb, A.; Khan, M.I. Recycled construction debris as concrete aggregate for sustainable construction materials. *Procedia Eng.* **2016**, *145*, 1518–1525. [CrossRef]
43. Koenders, E.; Pepe, M.; Martinelli, E. Compressive strength and hydration processes of concrete with recycled aggregates. *Cem. Concr. Res.* **2014**, *56*, 203–212. [CrossRef]
44. Surya, M.; Vvl, K.R.; Lakshmy, P. Recycled aggregate concrete for transportation infrastructure. *Procedia-Soc. Behav. Sci.* **2013**, *104*, 1158–1167. [CrossRef]
45. Tabsh, S.W.; Abdelfatah, A.S. Influence of recycled concrete aggregates on strength properties of concrete. *Constr. Build. Mater.* **2009**, *23*, 1163–1167. [CrossRef]
46. Etxeberria, M.; Vazquez, E.; Mari, A.; Barra, M. Influence of amount of recycled coarse aggregates and production process on properties of recycled aggregate concrete. *Cem. Concr. Res.* **2007**, *37*, 735–742. [CrossRef]
47. Wang, L.; Wang, J.; Qian, X.; Chen, P.; Xu, Y.; Guo, J. An environmentally friendly method to improve the quality of recycled concrete aggregates. *Constr. Build. Mater.* **2017**, *144*, 432–441. [CrossRef]
48. Saravanakumar, P.; Abhiram, K.; Manoj, B. Properties of treated recycled aggregates and its influence on concrete strength characteristics. *Constr. Build. Mater.* **2016**, *111*, 611–617. [CrossRef]
49. Zhan, B.; Poon, C.S.; Liu, Q.; Kou, S.; Shi, C. Experimental study on $CO_2$ curing for enhancement of recycled aggregate properties. *Constr. Build. Mater.* **2013**, *67*, 3–7. [CrossRef]
50. Gupta, P.K.; Rajhans, P.; Panda, S.K.; Nayak, S.; Das, S.K. Mix Design Method for Self-Compacting Recycled Aggregate Concrete and Its Microstructural Investigation by Considering Adhered Mortar in Aggregate. *Am. Soc. Civ. Eng.* **2019**, *32*, 04019371. [CrossRef]

51. *JGJ 52-2006*; Standard for Technical Requirements and Test Method of Sand and Crushed Stone (or Gravel) for Ordinary Concrete. China Building Industry Press: Beijing, China, 2006.
52. Liu, Y. *Research on Mechanical Properties and Penetration Resistance Mechanism of Steel Fiber Concrete*; University of Science and Technology of China: Shenzhen, China, 2006.
53. Wang, C.; Wu, K. Research on mechanical Properties of Steel fiber and carbon fiber concrete. *J. Build. Mater.* **2003**, *17*, 61–63.
54. Cheng, X. *Study on Strengthening Mechanism and Fracture Toughness of Steel Fiber Concrete*; Hohai University: Nanjing, China, 2005.
55. Zhu, Y. *Mechanical Properties of Steel Fiber Shotcrete and Its Application in Single Layer Lining of Tunnel*; Chongqing University: Chongqing, China, 2009.
56. Sun, M.Q.; Mao, Q.Z. Size effect and loading rate dependence of the pressure sensitivity of carbon fiber reinforced concrete. *J. Wuhan Univ. Technol.* **1998**, *13*, 58–61.
57. Craig, A.; William, G.; Habib, J.D. Testing and Analysis of Partially Composite Fiber Reinforced Polymer-Glulam-Concrete Bridge. *J. Bridge Eng.* **2004**, *19*, 1084–1092.
58. Tripathi, D.; Jones, F.R. Measurement of the Load-bearing Capability of the Fiber/Matrix Interface by Single Fiber Fragmentation. *Compos. Sci. Technol.* **1997**, *57*, 925–934. [CrossRef]
59. Guo, Y. *Research on Toughening Energy of Steel Fiber Concrete and Application of Toughness Characteristics in Calculation of Underground Structure*; Southwest Jiaotong University: Chengdu, China, 2008.
60. Lin, X.; Yang, G. *Steel Fiber High Strength and Ultra-High Strength Concrete*; Science Press: Beijing, China, 2002; pp. 35–90.
61. Gao, D.; Zhang, L.; Nokken, M.; Zhao, J. Mixture Proportion Design Method of Steel Fiber Reinforced Recycled Coarse Aggregate Concrete. *Materials* **2019**, *12*, 375. [CrossRef] [PubMed]
62. Ma, Y. *Design Method of Shotcrete Mix Ratio*; Northeast: College of Resources and Civil Engineering, Northeast University: Shenyang, China, 2013; pp. 84–86.
63. Guo, Y.; Li, Q. Simple design method for the mixture ratio of recycled coarse aggregate concrete. *J. Shenyang Jianzhu Univ.* **2017**, *33*, 1030–1038.
64. Hua, J.; Wangb, K.; Gauntb, J.A. Behavior and mix design development of concrete made with recycled aggregate from deconstructed lead-contaminated masonry materials. *Constr. Build. Mater.* **2013**, *40*, 1184–1192. [CrossRef]
65. Levy, S.M.; Helen, P. Durability of recycled aggregates concrete: A safe way tosustainable development. *Cem. Concr. Res.* **2004**, *34*, 1975–1980. [CrossRef]
66. Monteiro, P.J.M.; Helene, P.R.L.; Kang, S.H. Designing concrete mixtures for strength, elastic modulus and fracture energy. *Mater. Struct.* **1993**, *26*, 443–452.
67. Li, Q.; Gao, S.; Xue, S. *Green Concrete Technology*; China Building Materials Industry Press: Beijing, China, 2014.
68. Monalisa, B.; Bhattacharyya, S.K.; Minocha, A.K.; Deoliya, R.; Maiti, S. Recycled aggregate from C&D waste and its use in concrete-A break through towards sustainability in construction sector: A Review. *Constr. Build. Mater.* **2014**, *68*, 501–516.
69. Çakır, Ö. Experimental analysis of properties of recycled coarse aggregate (RCA) concrete with mineral additives. *Constr. Build. Mater.* **2014**, *68*, 17–25. [CrossRef]
70. Yu, J.; Liang, R.; Qin, Y.-J. Experimental study on the performance of C30 recycled coarse aggregate concrete. *Archit. Sci.* **2015**, *31*, 59–63.
71. Corinaldesi, V. Mechanical and elastic behavior of concretes made of recycled-concrete coarse aggregates. *Constr. Build. Mater.* **2010**, *24*, 1616–1620. [CrossRef]
72. Zhu, H.; Dai, J.; Bai, G. Test and Analysis of thermal conductivity of recycled concrete. *J. Build. Mater.* **2015**, *18*, 852–857.
73. Houria, M.; Oussama, K.; Hocine, O.; Berredjem, L.; Arabi, N. Influence of moisture conditioning of recycled aggregate on the properties of fresh and hardened concrete. *J. Clean. Prod.* **2013**, *54*, 282–288.
74. Sallehan, I.; Mahyuddin, R. Mechanical strength and drying shrinkage properties of concrete containing treated coarse recycled concrete aggregates. *Constr. Build. Mater.* **2014**, *68*, 726–739.
75. Cui, H.; Shi, X.; Memon, S.A.; Xing, F.; Tang, W. Experimental Study on the Influence of Water Absorption of Recycled Coarse Aggregates on Properties of the Resulting Concretes. *J. Mater. Civ. Eng.* **2015**, *27*, 04014138. [CrossRef]
76. Ferreira, L.; de Brito, J.; Barra, M.; Abbas, A. Influence of the pre-saturation of recycled coarse concrete aggregates on concrete properties. *Mag. Concr. Res.* **2011**, *63*, 617–627. [CrossRef]
77. Tam, V.; Gao, X.F.; Tam, C.M. Microstructural analysis of recycled aggregate concrete produced from two-stage mixing approach. *Cem. Concr. Res.* **2005**, *35*, 1195–1203. [CrossRef]
78. Guo, Y.; Li, Q.; Su, D.; Gao, S.; Yue, G. Formula for Predicting water consumption of recycled coarse aggregate concrete based on multiple factors. *Silic. Bull. Chin. Ceram. Soc.* **2008**, *37*, 1937–1940.
79. Zhou, A. Experimental study on the performance of common mortar for waste concrete production. *China Silic. Bull.* **2017**, *36*, 620–624.
80. Guo, Y.-X.; Li, Q.-Y.; Wang, W.-Q. Research on quality Improvement Technology of recycled coarse aggregate. *Concrete* **2015**, *6*, 134–138.
81. *GB/T 25177-2010*; Recycled Coarse Aggregate for Concrete. Ministry of Housing and Urban Construction of China: Beijing, China, 2010.
82. Zhang, C.; Song, F.; Liu, F. *Orial Handbooks of Building Construction*; China Building Industry Press: Beijing, China, 2011.
83. *DB37/T 5208-2021*; Technical Specification for Recycled Concrete Structures. Ministry of Housing and Urban and Rural Construction in People's Republic of China: Beijing, China, 2016.

84. Fang, Y. *Experimental Research on Stressing Performances of Recycled Concrete Simply-Supported Beams*; Central South University of Forestry and Technology: Changsha, China, 2009; pp. 14–18.
85. Yang, W. *Research on Mix Proportion and Physical Stress for Drying Shrinkage of Recycled Concrete Perforated Brick*; Zhengzhou University: Zhengzhou, China, 2007; pp. 24–31.
86. Hu, L.; Liang, J.-G. Effect of aggregate gradation on drying shrinkage of recycled concrete perforated brick. *New Build. Mater.* **2011**, *4*, 24–27.
87. Hao, T.; Liu, L. Research on shear strength of recycled aggregates concrete perforated brick masonry. *New Build. Mater.* **2016**, *7*, 51–53.
88. Zhang, X.; Deng, S.-C. Experimental research on unit water in recycled concrete. *Concrete* **2004**, *10*, 38–40.
89. Zhang, X. Calculation of water usage per unit volume of recycled concrete. *J. Cent. South For. Univ.* **2005**, *5*, 102–106.
90. Wang, M.; Yu, F.; Yin, C. Research on Additional Water of Mix Proportion for Recycled Aggregate Concrete. In Proceedings of the International Conference on Smart City and Systems Engineering (ICSCSE), Xiamen, China, 29–30 December 2018; pp. 328–331.
91. Kumar, A. *Thermal Spray Removal of Lead-Containing Paint of Steel Structures*; Construction Engineering Research Lab (ARMY): Champaign, IL, USA, 1999.
92. Kominsky, J.R. Field Demonstration of Lead-Based Paint Removal and Inorganic Stabilization Technologies. U.S. Environmental Protection Agency, Washington, DC, EPA/600/R-01/055 (NTIS PB2002-102037). 2001. Available online: https://cfpub.epa.gov/si/si_public_record_report.cfm?dirEntryId=99482&Lab=NRMRL (accessed on 5 July 2022).
93. Jacobs, D.E.; Mielke, H.; Pavur, N. The high cost of improper removal of lead-based paint from housing: A case report. *Environ. Health Perspect.* **2003**, *111*, 185–186. [CrossRef] [PubMed]
94. Garrels, R.M.; Christ, C.K. Solutions, minerals, and equilibria. *Harper Row N. Y.* **1965**, *32*, 34–37.
95. Brookins, D.G. *Eh–pH Diagrams for Geochemistry*; Springer: Berlin/Heidelberg, Germany, 1988.
96. Cao, X.; Ma, L.Q.; Chen, M.; Hardison, D.W.; Harris, W.G. Weathering of lead bullets and their environmental effects at outdoor shooting ranges. *J. Environ. Q.* **2003**, *32*, 526–634. [CrossRef]
97. ASTM (American Society for Testing and Materials). *Annual Book of ASTM Standards*; ASTM (American Society for Testing and Materials): Torrance, PA, USA, 2010.
98. Wang, K.; Gaunt, J.A.; Hu, J. Sequestering lead in paint by utilizing deconstructed masonry materials as recycled aggregate in concrete. *Strateg. Environ. Res. Dev. Prog. (SERDP) Proj. SI* **2008**, *44*, 1548.
99. Epa, U.S. Toxicity characteristics leaching procedure, Method 1311. *Test Methods Eval. Solid Waste* **1992**, *23*, 1989.
100. Kosmatka, S.H.; Kerkhoff, B.; Panarese, W.C. *Design and Control of Concrete Mixture*, 14th ed.; Portland Cement Association: Skokie, IL, USA, 2002.
101. Neville, A.M. *Properties of Concrete*, 4th ed.; ELBS and Longman: London, UK, 1996.
102. Hu, J.; Wang, K.; Gaunt, J.A. Sequestering lead by utilizing lead based paint contaminated masonry materials as recycled aggregate in concrete. *Resour Conserv Recy* **2010**, *54*, 1453–1460. [CrossRef]
103. California Code of Regulations. California State of Waste Extraction Test (WET) Procedures. 2005. Available online: https://govt.westlaw.com/calregs/Document/I84C9412C5B6111EC9451000D3A7C4BC3?viewType=FullText&originationContext=documenttoc&transitionType=CategoryPageItem&contextData=(sc.Default) (accessed on 5 July 2022).
104. Abbas, A.; Fathifazl, G.; Isgor, O.B.; Razaqpur, A.G.; Fournier, B. Proposed method for determining the residual mor-tar. *J. ASTM Int.* **2007**, *5*, 1–12. [CrossRef]
105. Fathifazl, G.; Abbas, A.; Razaqpur, A.G.; Isgor, O.B.; Fournier, B.; Foo, S. New mixture proportioning method for con-crete made with coarse recycled concrete aggregate. *J. Mater. Civ. Eng.* **2009**, *21*, 601–611. [CrossRef]
106. Belin, P.; Habert, G.; Thiery, M.; Roussel, N. Cement paste content and water absorption of recycled concrete coarse aggregates. *Mater. Struct. Constr.* **2013**, *47*, 1451–1465. [CrossRef]
107. *JGJ55-2011*; Code for Design of Common Concrete Mix. China Building Industry Press: Beijing, China, 2011.
108. Abbas, A.; Fathifazl, G.; Isgor, O.B.; Razaqpur, A.G.; Fournier, B.; Foo, S. Durability of recycled aggregate concrete designed with equivalent mortar volume method. *Cem. Concr. Compos.* **2009**, *31*, 555–563. [CrossRef]
109. Wenda, C.; Dong, C. *New Concrete and Its Application*; Jindun Press: Beijing, China, 2001.
110. Liu, J.; Huang, H. Influence of fly ash on the properties of steel fiber concrete. *Compr. Util. Fly Ash* **2002**, *1*, 44–45.
111. *DL/T5055-1996*; Technical Specification for Fly Ash in Hydraulic Concrete. Ministry of Electric Power Industry of China: Beijing China, 2011.
112. Wardeh, G.; Ghorbel, E.; Gomart, H. Mix design and properties of recycled aggregate concretes: Applicability of Eurocode 2. *Int. J. Concr. Struct. Mater.* **2015**, *9*, 1–20. [CrossRef]
113. EAnike, E.E.; Saidani, M.; Ganjian, E.; Tyrer, M.; Olubanwo, A.O. Evaluation of conventional and equivalent mortar volume mix design methods for recycled aggregate concrete. *Mater. Struct.* **2020**, *53*, 22. [CrossRef]
114. Gao, D.; Zhang, L.; Nokken, M. Compressive behavior of steel fiber reinforced- recycled coarse aggregate concrete with equivalent compressive strength. *Constr. Build. Mater.* **2017**, *141*, 235–244. [CrossRef]
115. Wedding, P.; Rasheeduzzafar; Khan, A. Recycled concrete-a source for new aggregate. *Cem. Concr. Aggregates* **1984**, *6*, 17–27. [CrossRef]
116. Ravindrajah, R.S.; Loo, Y.H.; Tam, C.T. Strength evaluation of recycled-aggregate concrete by in-situ tests. *Mater. Struct.* **1988**, *21*, 289–295. [CrossRef]

117. Katz, A. Properties of concrete made with RA from partially hydrated old concrete. *Cem. Concr. Res.* **2003**, *33*, 703–711. [CrossRef]
118. Bairagi, N.; Ravande, K.; Pareek, V. Behaviour of concrete with different proportions of natural and recycled aggregates. *Resour. Conserv. Recycl.* **1993**, *9*, 109–126. [CrossRef]
119. Padmini, A.K.; Ramamurthy, K.; Mathews, M.S. Influence of parent concrete on the properties of RAC. *Constr. Build. Mater.* **2009**, *23*, 829–836. [CrossRef]
120. Liu, C.; Fan, Z.Y.; Chen, X.N.; Zhu, C.; Wang, H.Y.; Bai, G.L. Experimental study on bond behavior between section steel and RAC under full replacement ratio. *KSCE J. Civ. Eng.* **2019**, *23*, 1159–1170. [CrossRef]
121. Elhakam, A.A.; Mohamed, A.E.; Awad, E. Influence of self-healing, mixing method and adding silica fume on mechanical properties of RAs concrete. *Constr. Build. Mater.* **2012**, *35*, 421–427. [CrossRef]
122. Kou, S.C.; Poon, C.S. Enhancing the durability properties of concrete prepared with coarse RA. *Constr. Build. Mater.* **2012**, *35*, 69–76. [CrossRef]
123. Fonseca, N.; de Brito, J.; Evangelista, L. The influence of curing conditions on themechanical performance of concrete made with recycled concrete waste. *Cem.Concr. Compos.* **2011**, *33*, 637–643. [CrossRef]
124. Collepardi, M.; Marcialis, A.; Turriziani, R. Penetration of chlo-ride ions into cement pastes and concretes. *J. Am. Ceram. Soc.* **1972**, *55*, 534–535. [CrossRef]
125. Monosi, S.; Moriconi, G.; Alverà, I.; Collepardi, M. Effect of water/cement ratio and curing time on chloride penetration into con-crete. *Mater. Eng.* **1989**, *1*, 483–489.
126. Saetta, A.V.; Scotta, R.V.; Vitaliani, R.V. Analysis of chloride diffusion into partially saturated concrete. *ACI Mater. J.* **1993**, *90*, 441–451.
127. Neville, A. Chloride attack of reinforced concrete: An overview. *Mater. Struct.* **1995**, *28*, 63–70. [CrossRef]
128. Ann, K.Y.; Moon, H.Y.; Kim, Y.B.; Ryou, J. Durability of recycled aggregate concrete using pozzolanic materials. *Waste Manag.* **2008**, *28*, 993–999. [CrossRef] [PubMed]
129. Corinaldesi, V.; Moriconi, G. Recycling of rubble from build-ing demolition for low-shrinkage concretes. *Waste Manag.* **2010**, *30*, 655–659. [CrossRef] [PubMed]
130. Poon, C.S.; Shui, Z.H.; Lam, L.; Fok, H.; Kou, S.C. Influence of moisture states of natural and recycled aggregates on the slump and compressive strength of hardened concrete. *Cem. Concr. Res.* **2004**, *34*, 31–36. [CrossRef]
131. Dhir, R.K.; Limbachiya, M.C.; Leelawat, T. Suitability of re-cycled concrete aggregate for use in BS 5328 designated mixes. *Proc. Inst. Civ. Eng. Struct. Build.* **1999**, *134*, 257–274. [CrossRef]
132. Santillán, L.R.; Villagrán Zaccardi, Y.A.; Benito, D.E.; Zega, C.J. Sulfate ingress in recycled concrete immersed in sodium sulfate solution for 10 years. In Proceedings of the Workshop on External Sulfate Attack; Laboratório Nacional de Engenharia Civil, Lisbon, Portugal, 3–4 November 2016.
133. Corinaldesi, V.; Moriconi, G. Influence of mineral additions on the performance of 100% recycled aggregate concrete. *Constr. Build. Mater.* **2009**, *23*, 2869–2876. [CrossRef]
134. Somna, R.; Jaturapitakkul, C.; Made, A.M. Effect of ground fly ash and ground bagasse ash on the durability of recycled aggregate concrete. *Cem. Concr. Compos.* **2012**, *34*, 848–854. [CrossRef]
135. Hwang, J.P.; Shim, H.B.; Lim, S.; Ann, K.Y. Enhancing the durability properties of concrete containing recycled aggregate by the use of pozzolanic materials. *KSCE J. Civ. Eng.* **2013**, *17*, 155–163. [CrossRef]
136. Mindess, S.; Young, J.F. *Concrete, 671*; Prentice-Hall: Englewood Cliffs, NJ, USA, 1981.
137. Mehta, P.K.; Monteiro, P.J.M. *Concrete: Microstructure, Properties, and Materials*, 3rd ed.; McGraw-Hill: New York, NY, USA, 2006; p. 600.
138. Nawy, E.G. *Concrete Construction Engineering Handbook*, 2nd ed.; CRC Press: Englewood Cliffs, NJ, USA, 2008; p. 1560.
139. Zega, C.J.; Di Maio, A.A. Recycled concrete exposed to high temperatures. *Mag. Concr. Res.* **2006**, *58*, 675–682. [CrossRef]
140. Zega, C.J.; Di Maio, A.A. Recycled concrete made with different natural coarse aggregates exposed to high temperature. *Constr. Build. Mater.* **2009**, *23*, 2047–2052. [CrossRef]
141. Enlin, M.; Jinxing, L.; Shuoshuo, X. Failure analysis and treatments of a loess tunnel being constructed in ground fissure area. *Eng. Fail. Anal.* **2022**, *134*, 106034.
142. He, S.; Lai, J.; Li, Y.; Wang, K.; Wang, L.; Zhang, W. Pile group response induced by adjacent shield tunnelling in clay: Scale model test and numerical simulation. *Tunn. Undergr. Space Technol.* **2021**, *120*, 104039. [CrossRef]
143. Li, Z.; Lai, J.; Li, Y.; Qiu, J.; Shi, Y.; Li, B.; Fan, F. Ground fissure disasters and mitigation measures for hazardsduring metro system construction in Xi'an, China. *Arabian J. Geosci.* **2022**, *15*, 5. [CrossRef]
144. Liu, X.G.; Ma, E.H.; Liu, J. Deterioration of an industrial reinforced concrete structure exposed to high temperatures and dry-wet cycles. Engineering Failure Analysis. *Eng. Fail. Anal.* **2022**, *135*, 106122. [CrossRef]
145. Shi, W.; Qiu, J.L.; Lai, J.X. Immersion mode and spatiotemporal distribution characteristic of water migration in loess tunnel. *Arabian J. Geosci.* **2022**, *15*, 654. [CrossRef]
146. Wang, X.; Fan, F.; Lai, J. Strength behavior of circular concrete-filled steel tube stub columns under axial compression: A review. *Constr. Build. Mater.* **2022**, *322*, 126144. [CrossRef]
147. Xu, S.; Ma, E.; Lai, J.; Yang, Y.; Liu, H.; Yang, C.; Hu, Q. Diseases Failures Characteristics and Countermeasures of Expressway Tunnel of Water-rich Strata: A Case Study. *Eng. Fail. Anal.* **2022**, *134*, 106056. [CrossRef]
148. Zhang, W.; Lai, T.; Li, Y. Risk Assessment of Water Supply Network Operation Based on ANPFuzzy Comprehensive Evaluation Method. *J. Pipeline Syst. Eng. Pract.* **2022**, *13*, 04021068. [CrossRef]

149. Zhang, G.-L.; Zhang, W.-J.; Li, H.-L.; Cao, W.-Z.; Wang, B.-D.; Guo, W.-S.; Gao, P. Waterproofing behavior of sealing gaskets for circumferential joints in shield tunnels: A full-scale experimental investigation. *Tunn. Undergr. Space Technol.* **2020**, *108*, 103682. [CrossRef]
150. Liu, C.; Zhou, S.; Yu, C.; Ma, E.; Kong, F.; Tang, X.; Gao, X.; Zhang, X.; Lai, J. Damage behaviours of new-to-old concrete interfaces and a damage prediction model of reinforced concrete. *Eur. J. Environ. Civ. Eng.* **2022**, *164*, 1981459. [CrossRef]
151. Niu, F.Y.; Cai, Y.C.; Yang, T. Unfavorable Geology and Mitigation Measures for Water Inrush Hazard during Subsea Tunnel Construction: A Global Review. *Water* **2022**, *14*, 1592. [CrossRef]
152. Xu, S.; Nowamooz, H.; Lai, J. Mechanism, Influencing Factors and Research Methods for Soil Desiccation Cracking: A Review. *Eur. J. Environ. Civ. Eng.* 2022; *in press*.
153. Qin, Y.; Lai, J.; Yang, T.; Zan, W.; Feng, Z.; Liu, T. Failure analysis and countermeasures of a tunnel constructed in loose granular stratum by shallow tunnelling method. *Eng. Fail. Anal.* **2022**, *141*, 106667. [CrossRef]
154. Liu, C.; Liu, Y.; Chen, Y. A state-of-the-practice review of three-dimensional laser scanning technology for tunnel distress monitoring. *J. Perform. Constr. Facil.* **2022**, *152*, 107752.
155. Wang, Z.C.; Cai, Y.C.; Fan, Y.; Lai, J.X.; Kong, X.G. Local buckling characteristic of hollow π-type steel-concrete composite support of loess tunnel in hilly-gully region. *Eng. Fail. Anal.* **2022**, *143*, 106669.
156. Qin, Y.; Qiu, J.; Lai, J.; Liu, F.; Wang, L.; Luo, Y.; Liu, T. Seepage Characteristics in Loess Strata Subjected to Single Point Water Supply. *J. Hydrol.* **2022**, *609*, 127611. [CrossRef]
157. Yan, Y.F.; Huang, Q.B.; Liu, T. Failure analysis and deformation mechanism of segmented utility tunnels crossing ground fissure zones with different intersection angles. *Eng. Fail. Anal.* **2022**, *139*, 106456. [CrossRef]
158. Yan, Y.F.; Huang, Q.B.; Wang, Y.L. Failure analysis of urban open-cut utility tunnel under ground fissures environment in Xi'an, China. *Eng. Fail. Anal.* **2021**, *127*, 105529. [CrossRef]
159. He, S.Y.; Lai, J.X.; Zhang, C.P. Damage behaviors, prediction methods and prevention methods of rockburst in 13 deep traffic tunnels in China. *Eng. Fail. Anal.* **2021**, *121*, 105178. [CrossRef]
160. Fang, Q.; Liu, X.; Fang, Q.; Zeng, K.H.; Zhang, X.D.; Zhou, M.Z.; Du, J.M. Centrifuge modelling of tunnelling below existing twin tunnels with different types of support. *Undergr. Space* **2022**. [CrossRef]
161. Liu, X.G.; Zhang, W.P.; Gu, X.L.; Ye, Z.W. Assessment of Fatigue Life for Corroded Prestressed Concrete Beams Subjected to High-Cycle Fatigue Loading. *J Struct. Eng.* 2022; *in press*.
162. Fan, H.B.; Liu, T.; Zhang, S.Y.; He, H.J.; Zhu, Z.G.; Zhu, Y.Q.; Gao, X.Q. Effects of Jet Grouting Piles on Loess Tunnel Foundation with Centrifugal Model Tests. *Int. J. Geomech.* 2022; *in press*.